Transimpedance Amplifier Design and Performance Comparison for Photoelectric Cells

Muhammed Taha KAVLAK[1], Umut Engin AYTEN[2]

[1,2]Department of Electronics & Communication Engineering
Yildiz Technical University
Istanbul, Turkey
[1]taha.kavlak@std.yildiz.edu.tr
[2]ayten@yildiz.edu.tr

Abstract

In this study, a transimpedance amplifier design is implemented by using a current feedback operational amplifier as an active element for photoelectric cells used for purposes such as particle counters, flow cytometry and smoke detection. The performance of the designed circuit and the commonly used transimpedance amplifier circuit by using a commercially available operational amplifier were experimentally investigated on a measurement setup in accordance with industry accepted standards. In experiments, a reference measurement system and an aerosol generator which is capable of producing aerosol particles in accordance with the requirements of the standards were used. Firstly, the magnitudes of the currents which were generated by the photodiode, were measured by the reference measurement system at different pressure settings of the aerosol generator, thus, the generated currents at different aerosol generator set were determined. The sensor current magnitudes obtained at different gas particle densities were applied to the designed transimpedance amplifier circuits and the obtained results were compared. The relationship between the output voltage values of the transimpedance amplifier circuits and the gain resistance values was examined using simulation results with PSPICE and experimental results obtained with the test circuits carried out for this study.

1. Introduction

Photoelectric measurement cells are used for purposes such as particle counting, flow cytometry, and smoke detection [1, 2]. The one of the most common measurement technique for photoelectric cells relies on the generated current of the photodiode which is activated by the scattered light from the particles (aeresols). The most critical part is the precise measurement of the current magnitude at the output of the photodiode element caused by the scattered light which depends on the aerosol density. In this structure, the current magnitudes generated by the photodiode element are very low. These current values need to be amplified and converted to voltage values that can be used by the electronic hardware. For this purpose, transimpedance amplifier (TIA) circuits should be used that the input and output of the amplifier are current and voltage, respectively.

Various TIA circuit structures were designed by using different active elements have been proposed in the literature. These circuits are designed by using operational amplifiers (OpAmp) [2], second generation current carriers (CCII) [3], second generation voltage carriers (VCII) [4], operational transconductance amplifiers (OTA) [5], current differential transresistance amplifier (CDTRA) [6] with different active elements.

In the literature, the comparison of resistive and capacitive TIA circuits is given in [7]. However, in this study, the comparison is based on the circuit structures realized with the operational amplifier active element. In [8], a current mode circuit design with current input and voltage output was given and compared with a TIA structure with operational amplifier active element and shunt feedback. However, the study is given as a simulation result on the CMOS circuit structure.

In this study, a TIA circuit design was carried out by using the current feedback operational amplifier to convert the current which was generated by photodiode element into voltage magnitude according to the change of aerosol density in the photoelectric cell. This circuit is experimentally compared with the commonly used TIA circuit which is designed with operational amplifier.

In Chapter 2, TIA circuit with operational amplifier and CFOA are given. In addition, the relationship between the output voltage values of the TIA circuits and the gain resistance value and the frequency characteristics of the circuits were examined using PSPICE simulation results. In Chapter 3, the experimental results of the circuits are given. The results are explained in Chapter 4.

2. Transimpedance Amplifier

In the TIA circuit designed in this study, the commercially available AD844 [9] integrated circuit was used as Current Feedback Operational Amplifier (CFOA) active element. OPA2191 OpAmp [10] integrated circuit was used for TIA circuit with operational amplifier. In both TIA circuits, there are two stage of analog circuit structures connected in cascade. On the first stage, the current magnitude is converted to voltage, and on the second stage, the voltage magnitude is amplified. The gain resistors for both structures are chosen of equal.

2.1. CFOA Based Transimpedance Amplifier

The circuit symbol and ideal equivalent circuit model of the CFOA active element are given in Fig. 1 and the definition relations are given by Eq. (1). Here, α is the current gain, β and γ are the voltage gain expressions. Ideally $\alpha = \beta = \gamma = 1$.

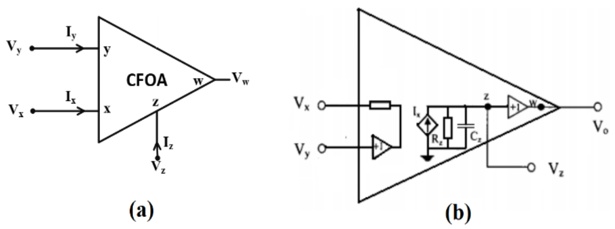

Fig. 1. CFOA a) circuit symbol b) ideal equivalent circuit

$$\begin{bmatrix} I_y \\ I_z \\ V_x \\ V_w \end{bmatrix} = \begin{bmatrix} 0 & 0 & 0 \\ \alpha & 0 & 0 \\ 0 & \beta & 0 \\ 0 & 0 & \gamma \end{bmatrix} \begin{bmatrix} I_x \\ V_y \\ V_z \end{bmatrix} \quad (1)$$

The TIA circuit structure using the CFOA active element is given in Fig. 2. The relationship between input and output of the circuit which is given in Fig. 2 is illustrated Eq. (2).

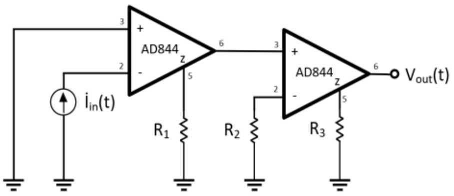

Fig. 2. CFOA Based Transimpedance Amplifier Circuit

$$V_{out} = -i_{in} \frac{R_1 R_3}{R_2} \quad (2)$$

2.2. OpAmp Based Transimpedance Amplifier

The general circuit structure of the shunt feedback transimpedance amplifier structure realized with the OpAmp active element is illustrated in Fig. 3.

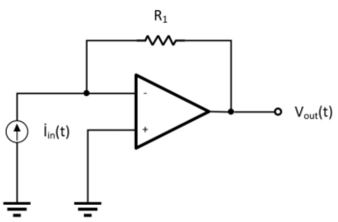

Fig. 3. Shunt Feedback Transimpedance Amplifier

In this circuit structure, the output voltage expression is as given in Eq. (3).

$$V_{out} = -i_{in} R_1 \quad (3)$$

In the OPAMP structure, the current flowing to the input terminals has an effect on the gain. Considering this effect, OPA2191 OPAMP element with a low input current of ±5 pA was selected for this study.

In practice, a capacitor element must be added in parallel with the feedback resistor for stable operation. This capacitor also determines the minimum gain-bandwidth (GBW) of the OPAMP element[11].

$$GBW > \frac{C_i + C_f}{2\pi R_f (C_f)^2} \quad (4)$$

In this equation, C_i is input capacitance, C_f is feedback capacitance and R_f is feedback resistance.

The TIA circuit structure, which was used in the experimental part of this study, is given in Fig. 4. When the circuit is analyzed in DC conditions, the expression for the output voltage is obtained as given in Eq. (5).

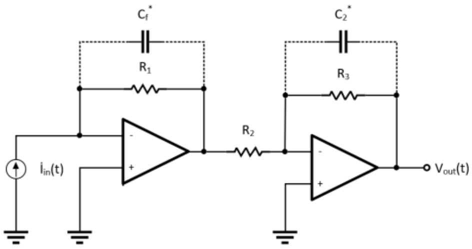

Fig. 4. OpAmp Based Transimpedance Amplifier Circuit

$$V_{out} = i_{in} \frac{R_1 R_3}{R_2} \quad (5)$$

2.3. Test Circuits

Prototype test boards were prepared for CFOA and OpAmp TIA circuits. The connection between the TIA circuits and the sensor is a BNC connector. The circuits operate with ±12V DC symmetrical supply. The pictures of the test circuits are given in Fig. 5.

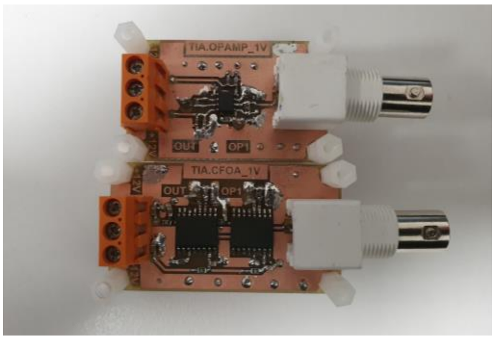

Fig. 5. Test boards prototype

2.4. Simulation Results

In the given circuits, R_2 = 2 kΩ, R_3 = 100 kΩ was chosen. For the R_1 resistor, simulation in PSPICE environment and experimental tests were realized by using 100 kΩ, 240 kΩ, 510 kΩ, 750 kΩ and 1 MΩ resistors, respectively. In order for the experiment and simulation to be carried out with the same input current, 104 nA (±5%), which was read on the reference measuring device as input current, was applied to the input of the circuit in the simulator.

The pulse duration of the input current was chosen to be 1ms. In terms of aerosol analysis, it is possible to sample approximately 20 aerosol clouds in the experimental set for 1 ms. Thus, analysis of a larger number of particles is possible.

The simulation results of the variation of the output voltage according to different R_1 resistors are given in Fig. 6 and 7. Due to the DC level occurs in the circuit using CFOA, the simulation results were obtained by filtering the DC level.

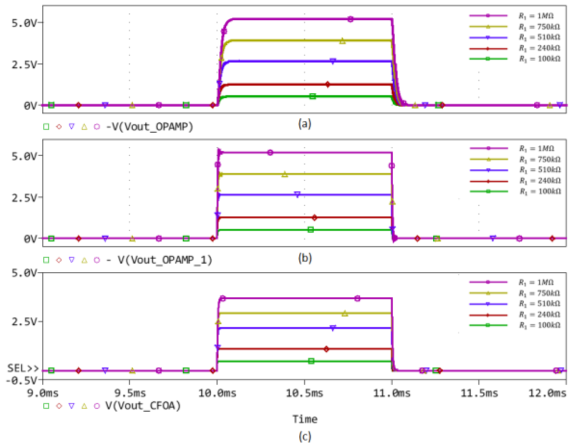

Fig. 6. Transient Simulation Results (Full pulse) (a) OPAMP TIA with using feedback capacitor (b) OPAMP TIA without using feedback capacitor (c) CFOA TIA

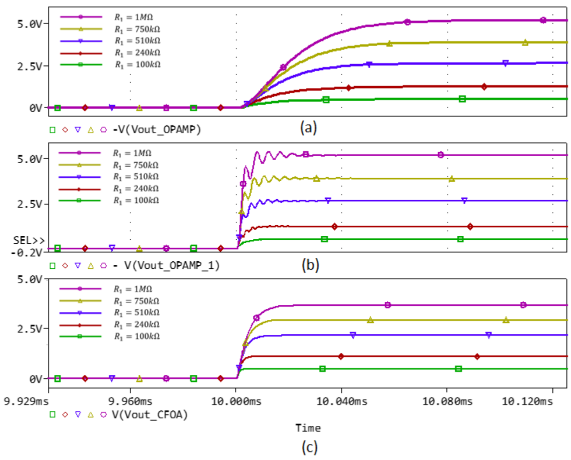

Fig. 7. Transient Simulation Results (Beginning of the pulse) (a) OPAMP TIA with using feedback capacitor (b) OPAMP TIA without using feedback capacitor (c) CFOA TIA

It is seen that there is a distortion in the pulse form in the OPAMP circuit where the feedback capacitor is not used.

The frequency characteristics of the given circuits are given in Fig. 8, 9 and 10. The cut-off frequencies of TIA circuits for different gain resistance values are given in Table 1.

Table 1. Cut-off Frequencies of TIA Circuits

TIA Circuit	Gain Resistors (Ω)				
	100 k	**240 k**	**510 k**	**750 k**	**1 M**
Opamp without Feedback Cap.	58.8 kHz	60.5 kHz	62.6 kHz	66.7 kHz	69.8 kHz
Opamp with Feedback Cap.	12.5 kHz	12.1 kHz	11.0 kHz	10.0 kHz	8.9 kHz
CFOA	194.5 kHz	112.4 kHz	63.2 kHz	46.5 kHz	37.9 kHz

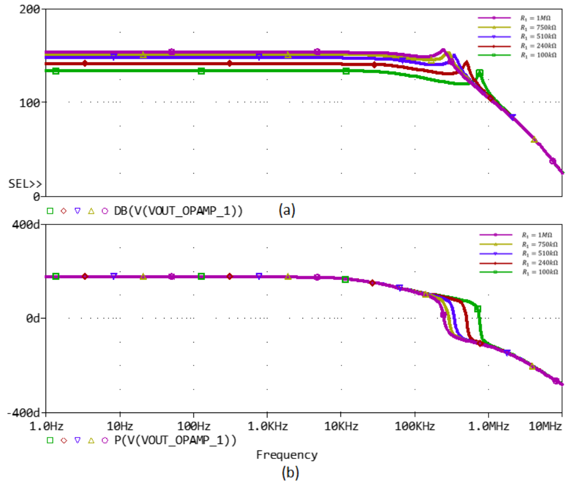

Fig. 8. Frequency Characteristic of OPAMP TIA without using feedback capacitor (a) Gain (b) Phase

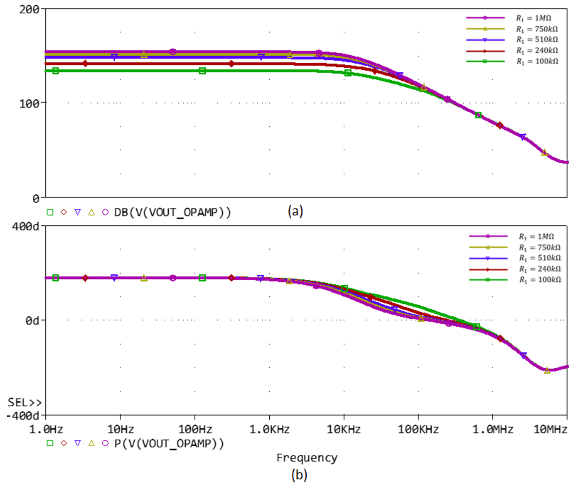

Fig. 9. Frequency Characteristic of OPAMP TIA with using feedback capacitor (a) Gain (b) Phase

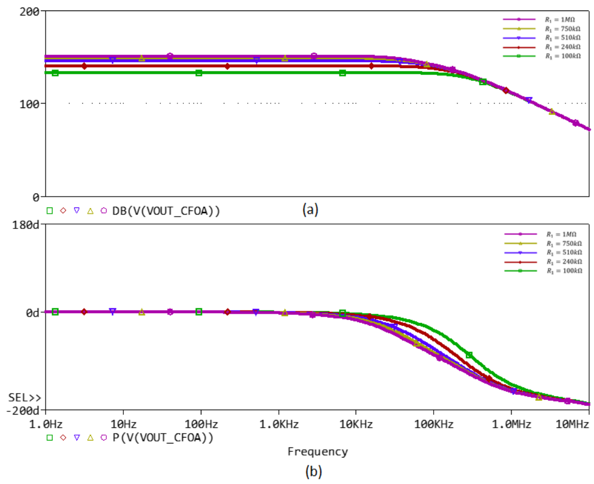

Fig. 10. Frequency Characteristic of CFOA TIA (a) Gain (b) Phase

3. Experimental Results

In this section, first of all, it is experimentally examined how the change in gain resistance effects of the amplifier. As a result of these measurements, the appropriate gain resistor value was determined so that the circuits would operate within the linear operating range. Then, the created circuits were compared experimentally on the photoelectric cell aerosol measurement system used in the industry for particle counting, flow cytometry, and smoke detection purposes.

Experimental results, simulation results and theoretical calculations of the gain resistor effect on the output voltage are as given in Table 2 and Fig. 11. All results were obtained for 104 nA input current.

Table 2. TIA Gain Resistor Test Results

R_1 (Ω)	***Output Voltage (V)***				
	Theoretical Calculation	***Simulation***		***Experiment***	
		CFOA	***OPAMP***	***CFOA***	***OPAMP***
100 k	0.504	0.472	0.520	0.472	0.484
240 k	1.248	1.084	1.248	1.110	1.120
510 k	2.652	2.126	2.652	2.180	2.340
750 k	3.900	2.926	3.900	2.940	3.400
1 M	5.200	3.658	5.200	3.800	4.360

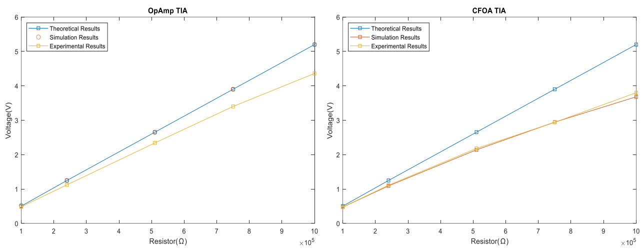

Fig. 11. Test results comparison graphs

According to the results, it is clear that the linearity of the circuit realized with CFOA is getting worse according to the gain. The obtained simulation results and experimental results overlap with each other. According to the results, the R_1 resistance was chosen as 510 kΩ, taking into account the results. C_f = 10 pF, C_2 = 100 pF were chosen to increase the stability of the OpAmp.

After selecting the gain resistor value, its comparison in two different TIA circuits connected to the photodiode sensor in a photoelectric cell was examined experimentally. Reference devices and optical measuring cell included in the study [1] were used in the measurement setup. The block diagram of the system is shown in Fig. 12.

In the experiments, the density of the aeresol was controlled by TOPAS ATM 228 aerosol generator [12]. Keeping the photodiode current constant at photoelctric cell is succeeded by using aerosol generator at different stages. Thus, the repeatable and reproducible tests were performed. According to EN 54-7 standard, paraffin oil was used to create aerosol with the aerosol generator [13].

Different current values were generated in the photoelectric cell by the different aerosol densities which were produced at different stages of the aeresol generator. Aerosol densities were established at 300, 350, 400, 450 and 500 pressure stages of the aerosol generator, respectively. The sensor current generated at different aerosol densities was first measured with the Thorlabs PDA200C [14] reference measurement device on an oscilloscope and the results were recorded. All experimental results were plotted on the MATLAB program. During the experiments, the light source in the photoelectric cell was driven with a pulse width of 1ms.

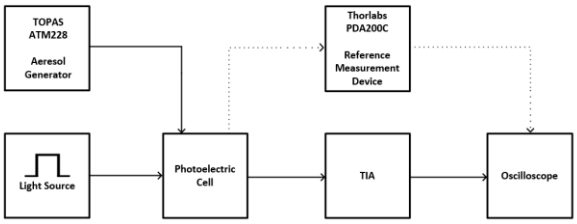

Fig. 12. Measurement system block diagram

The results of the reference device output voltage are given in Fig. 13. The current values corresponding to the measured values were calculated according to the step gain of the device and given in Table 3. Measurement values include ±5% error margin.

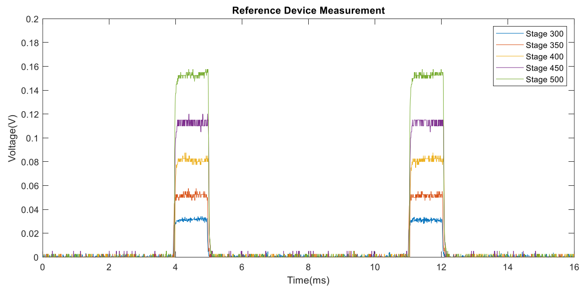

Fig. 13. Reference measurement device output

Table 3. Results of reference device measurements

Device Stage	***300***	***350***	***400***	***450***	***500***
Measured Voltage (mV)	30	50	80	110	150
Calculated Currents (nA)	30 ± 1.5	50 ± 2.5	80 ± 4	110 ± 5.5	150 ± 7.5

After measuring the current values on the sensor in the cell, the current output of the photodiode was applied to the CFOA and OpAmp TIA circuits respectively and the results were recorded on the oscilloscope. To eliminate DC level, the measurements were carried out with AC coupling. The obtained results are given in Fig. 14. In the circuit with OPAMP, the output signal has negative amplitude. The OPAMP signal is inverted in the graph and plotted as positive amplitude.

The experimental results are given in Table 4. The table shows the output voltages obtained in response to the input currents applied to the circuits.

Table 4. Results of Tia Circuit Measurements

Current Value (nA)		***30***	***50***	***80***	***110***	***150***
Measured Voltage (V)	**CFOA**	0.77	1.18	1.77	2.53	3.32
	OPAMP	0.70	1.22	1.85	2.75	3.55

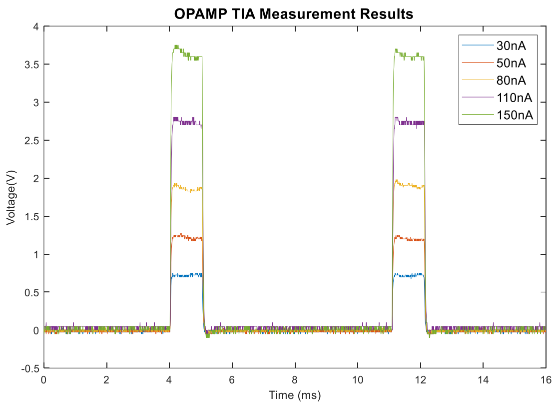

(a)

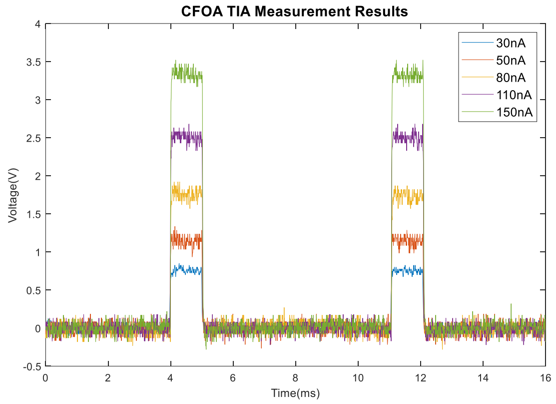

(b)

Fig. 14. Experimental Results (a) OPAMP TIA (b) CFOA TIA

4. Conclusions

In this study, the constant current in the order of nanoamperes of the photodiode which was generated in the photoelectric cell by applying aerosol created by the aerosol generator, was registered to CFOA and OpAmp TIA circuits with equal gain values. The TIA circuit using CFOA proposed in this study, has not been encountered in the literature. It was obtained through amplifier circuits and basic analog circuit structures using CFOA and CCII. In order to carry out the experimental study, the physical realization of the circuits was made. The sensor current was measured with a reference device and the sensor current was calculated within the margin of error. Obtained test results are given comparatively. All experiments were performed in a physical measurement setup that conformed to industry accepted standards. Therefore, the TIA circuit proposed in this study can be used in industry for particle counting, flow cytometry and smoke detection.

In the circuit structure realized with CFOA, feedback capacitor and feedback resistor are not used. Therefore, there is no factor limiting the bandwidth. In this form, the circuit using CFOA and the feedback circuit with OpAmp were compared in a practical experimental environment. With this study, it has been shown that the CFOA TIA circuit structure can be used as an alternative to the classical OpAmp circuit structure. AD844 was used as a commercial product in the CFOA TIA structure. It is possible to obtain better results here by using advances CMOS technology.

5. References

[1] Özyurt, Osman. "Methods of Classifying Aerosol Types by Using Scattering of Light." 2022 International Conference on INnovations in Intelligent SysTems and Applications (INISTA). IEEE, 2022.

[2] Shao, Wenjia, Hongjian Zhang, and Hongliang Zhou. "A new particle sensor based on true RMS value measurement." 2016 IEEE International Instrumentation and Measurement Technology Conference Proceedings. IEEE, 2016.

[3] Nastro, Alessandro, et al. "A current-mode transimpedance amplifier for capacitive sensors." Proceedings. Vol. 2. No. 13. MDPI, 2018.

[4] García-Montesdeoca, José C., Juan A. Montiel-Nelson, and Javier Sosa. "High Gain, Low Noise and Power Transimpedance Amplifier Based on Second Generation Voltage Conveyor in 65 nm CMOS Technology." Sensors 22.16 (2022): 5997.

[5] Serri, Mahziar, and Saeed Saeedi. "Ultra-low-noise TIA topology for MEMS gyroscope readout." AEU-International Journal of Electronics and Communications 118 (2020): 153145.

[6] Dikbaş, Mehmet Cem, and Umut Engin Ayten. "Current and transimpedance mode instrumentation amplifier using a single new active component named CDTRA." AEU-International Journal of Electronics and Communications 91 (2018): 24-36.

[7] Rajabzadeh, Mahdi, et al. "Comparison study of integrated potentiostats: Resistive-TIA, capacitive-TIA, CT σδ modulator." 2018 IEEE International Symposium on Circuits and Systems (ISCAS). IEEE, 2018.

[8] Trabelsi, Abdelaziz, and Mounir Boukadoum. "Comparison of two CMOS front-end transimpedance amplifiers for optical biosensors." IEEE Sensors Journal 13.2 (2012): 657-663.

[9] Analog Devices, 60 MHz 2000 V/us Monolithic Op Amp, AD844 datasheet, Rev. F., 2009.

[10] OPAx191 36-V, Low-Power, Precision, CMOS, Rail-to-Rail Input/Output, Low Offset Voltage, Low Input Bias Current Op Amp. Texas Instruments, Dallas, TX, USA, Dec. 2015.

[11] Caldwell, John. "Transimpedance Amplifiers: What Op Amp Bandwidth do I Need?." Texas Instrum., Dallas, TX, USA, Tech. Rep (2014).

[12] “Topas ATM228 Aerosol Generator Datasheet”, Accessed on: Sept. 03, 2022. [Online] Available: https://www.topas-gmbh.de/en/products/generation/product/atm-228

[13] Fire detection and fire alarm systems smoke detectors, Point smoke detectors that operate using scattered light, transmitted light or ionization, EN 54-7, 2018

[14] Thorlabs Inc., PDA200c Benchtop Photodiode Amplifier, Accessed on: Sept. 06, 2022. [Online] Available: https://www.thorlabs.com/_sd.cfm?fileName=15987-D02.pdf&partNumber=PDA200C